

SN 1996N - A type Ib supernova at late phases*

Jesper Sollerman^{1,2}, Bruno Leibundgut¹, and Jason Spyromilio¹

¹ European Southern Observatory, Karl-Schwarzschild-Strasse 2, D-85784 Garching bei München, Germany

² Stockholm Observatory, S-133 36 Saltsjöbaden, Sweden

Received 30 March 1998 / Accepted 10 June 1998

Abstract. We present photometric and spectroscopic observations of the Type Ib supernova (SN Ib) 1996N in NGC 1398. The supernova has been observed at several occasions between 179 and 337 days after discovery. The light curves in V , R and I have decline rates of 1.67 ± 0.23 , 1.72 ± 0.10 and 1.93 ± 0.24 mag $(100\text{d})^{-1}$ respectively, substantially faster than the decay rate of ^{56}Co . The late light curves of SN 1996N are rather similar to the light curves of SN 1993J, and the decline is consistent with simple models of a radioactively powered supernova, where the γ -rays are leaking out of the ejecta. SN 1996N appears to be underluminous compared to SN 1993J, possibly indicating that less ^{56}Ni was ejected in the explosion, but uncertainties in intrinsic absorption prevents us from definite conclusions.

The late time spectra of SN 1996N are similar to spectra of other SNe Ib/c, and are dominated by [O I] $\lambda\lambda 6300, 6364$, [Ca II] $\lambda\lambda 7291, 7324$, and the Ca II near-IR triplet. In particular, these spectra closely resemble those of SN 1993J. We speculate about the possibility that the broad emission feature seen redward of [O I] $\lambda 6364$ in SN 1996N could be due to $\text{H}\alpha$, as it was in SN 1993J. In this scenario, small amounts of hydrogen might go unnoticed in the early spectra of SN Ib/c. Later on, when the SN continuum has faded, the hydrogen layer might be re-excited, thus revealing its existence.

Finally, we note that the emission lines of SN 1996N are blueshifted by ~ 1000 km s^{-1} . With the scenarios proposed for the blueshifts in SN 1993J in mind, we discuss the possible cause for the shifts in SN 1996N. The lineshifts may in fact indicate large scale asymmetries in the supernova explosion, rather than the formation of dust at early epochs.

Key words: supernovae: general – supernovae: SN 1996N – galaxies: individual: NGC 1398

1. Introduction

Core collapse supernovae (SNe) come in various appearances. During the early phases of the explosions, the emission is dom-

inated by the shock-excited material in the outer layers of the exploding star. Once the ejecta have expanded to become optically thin, we can study the inner layers of the progenitor star and the energy input into the debris. Thus, the classification scheme, which is based on the spectral appearance near maximum light (Harkness & Wheeler 1990, Filippenko 1997), does not necessarily encapsulate the appearance of the supernova at late phases. This has been demonstrated by transition objects like SN 1993J and SN 1987K. These SNe showed hydrogen-dominated spectra, characteristic of Type II supernovae (SNe II), near maximum, but changed to oxygen and calcium dominated spectra in their nebular phase. Their late spectra were thus similar to the spectra of hydrogen-deficient Type Ib and Type Ic supernovae.

The existence of SNe transforming from SNe II to SNe Ib/c clearly indicates a relationship between these subclasses of supernovae. In this scenario, SNe Ib/c are produced by core collapse of massive stars, just as SNe II, except that their progenitors were stripped of their H (SN Ib) and possibly He (SN Ic) envelopes prior to the explosion, either by mass transfer to a companion (Nomoto et al. 1994) or via winds (Woosley et al. 1993). The transition objects are thus believed to have progenitors were most, but not all, hydrogen was removed before the explosion.

Apart from differences in their spectra, supernovae also show variations in their light curves. At late times SN II generally follow the decay rate of ^{56}Co (Turatto et al. 1990; Patat et al. 1994), whereas some SNe Ib/c decay faster (Wheeler & Harkness 1989; Clocchiatti & Wheeler 1997). This is attributed to differences in optical depth for the γ -rays from the ^{56}Co decay. The faster decline rate of SNe Ib/c is thus due to a lower optical depth, which in turn is related to the smaller ejecta mass of these SNe. So far, however, only few core-collapse supernovae have been observed at late phases (> 6 months after explosion; Patat et al. 1994).

While observations at late phases, when the SN is faint, are clearly more difficult, spectra at late epochs probe deeply into the core of the exploding star, and the expansion leads to an optically thin nebula where the spectral interpretation is easier. For SNe Ib/c the absence of a large hydrogen envelope creates an even cleaner window into the heart of supernova nucleosynthesis.

* Based on observations collected at the European Southern Observatory, La Silla, Chile.

Correspondence to: jesper@astro.su.se

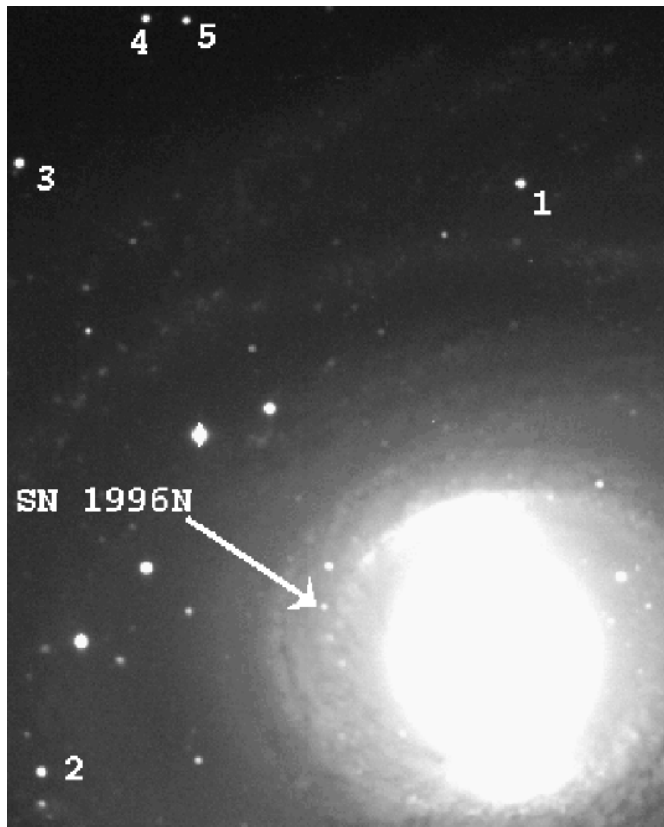


Fig. 1. SN 1996N in NGC 1398. North is up and east to the left. This V-image was taken with the ESO/MPI 2.2m telescope in October 1996, 221 days after discovery. The comparison stars are numbered and the supernova is marked with an arrow.

Supernova 1996N was discovered on March 12.5, 1996, in the large, barred spiral galaxy NGC 1398 (Williams & Martin 1996). The supernova is located $46''$ east and $12''$ north of the center of the galaxy (Fig. 1). Nothing was visible at this location on February 16. An early spectrum obtained on March 23.4 showed this to be a SN Ib/c about two weeks past maximum (Germany et al. 1996), and Van Dyk et al. (1996) reported a radio detection of the supernova at 3.6 cm on April 2.0 with the VLA. Here we report on optical observations of SN 1996N taken several months after explosion. We have observed the supernova on five occasions with several La Silla telescopes. These observations are part of a long-term program to study core-collapse supernovae at late phases.

2. Observations and reductions

2.1. Photometry

Our photometric data were obtained on five epochs between September 1996 and February 1997. The log of the photometry is given in Table 1. The data were bias subtracted and flat fielded using tasks in IRAF¹. The transformations to standard magnitudes were obtained from observations of four Landolt (1992) standard fields and one E-field of Graham (1982) on the night

Table 1. Supernova 1996N - log of photometry observations.

Julian Date 2450000+	UT Date	Telescope/ Instrument	Filter
333.8	7.3 Sep. 96	3.6m/EFOSC1	R
375.8	19.3 Oct. 96	1.54m/DFOSC	B,V,I
376.0	19.5 Oct. 96	2.2m/EFOSC2	R
433.7	16.2 Dec. 96	2.2m/EFOSC2	V,R,I
461.6	13.1 Jan. 97	2.2m/EFOSC2	V,R,I
491.5	12.0 Feb. 97	3.6m/EFOSC1	V,R
744.8	23.3 Oct. 97	NTT/EMMI	V,R,I

of January 13, 1997. We solved for extinction and color corrections using the IRAF task PHOTCAL. Several local comparison stars were calibrated in the field. The supernova magnitudes of all other nights were measured relative to these stars. The comparison stars are marked in Fig. 1 and their magnitudes are given in Table 2.

Obtaining magnitudes of a fading point source on a complex background is not a simple task. Normal aperture photometry is often not adequate (Turatto et al. 1993). We tried two different approaches: Point spread function (PSF) fitting and galaxy template subtraction.

For the PSF fitting we used DoPhot (Schechter et al. 1993). This software package obtains magnitudes by PSF fitting, using an empirical PSF obtained from one of the stars in the field. A problem with this method is the variability of the PSF across the field, seen in several of our images. This variability is probably due to the rather complex optics of the EFOSC-type instruments (Magain et al. 1992) and means that systematic errors can be introduced by forcing the fit of the empirical PSF star onto the supernova. Subtractions of the fitted PSFs do show rather large residuals.

To minimize these errors each magnitude was obtained using two different standard stars, number 1 and 2 in Fig. 1, for the empirical PSF. These stars are well exposed, relatively isolated and located at opposite sides of the supernova. The differences for the measured supernova magnitudes are actually rather small, with a standard deviation of less than 0.05 magnitudes in R .

To check the performance of DoPhot on the complex background we also extracted the magnitudes of a star close to the supernova (offset from SN 1996N by $1''.2$ W , $10''.5$ N), and obtained 19.21 ± 0.04 in R . The error is the standard deviation of the magnitudes for the five epochs and gives a handle on the consistency of our measurements and a hint to the errors of the supernova magnitudes, at least for the earlier epochs.

As an independent check on some of the systematic errors we also tried the galaxy template subtraction method. On October 23.3, 1997, we obtained deep images of NGC 1398 in V , R and I with the ESO/NTT. Inspection of these images showed

¹ IRAF is distributed by the National Optical Astronomy Observatories, which are operated by the Association of Universities for Research in Astronomy, Inc., under cooperative agreement with the National Science Foundation.

Table 2. Magnitudes of comparison stars.

	V	R	I
1	18.00	17.56	17.10
2	18.39	17.49	16.60
3	18.07	17.37	16.73
4	18.99	18.48	17.98
5	19.42	18.67	17.96

Magnitudes for the comparison stars marked in Fig. 1. The uncertainties are about 0.05 magnitudes.

that the supernova had faded from visibility, the 3σ upper limit being 23.0 magnitudes in *R*.

For each of our previous frames the NTT images were aligned and rescaled using standard IRAF tasks. Thereafter the sky was subtracted from the images and the NTT image was scaled to match the flux of the other image as measured in the comparison stars.

Before subtracting the images we had to assess the problem of different PSFs. We did this in two different ways both starting with the construction of a PSF with the IRAF/DAOPHOT task PSF, using three nearby stars.

One way to proceed is to deconvolve the PSF having larger FWHM with the other PSF using the Lucy-Richardson deconvolution task LUCY. Thereafter the image with the smaller PSF was convolved with the kernel from the above deconvolution. An alternative approach is to deconvolve both images with their respective PSF using a relatively large number of iterations. Thereafter the deconvolved images are smoothed with a Gaussian, resulting in images where all stars are nice Gaussians with preserved flux. The frames were then subtracted and the subtracted frame was measured with aperture photometry. The template method is, however, also likely to introduce errors. For example, we have used four different telescope systems with different color response. Also, the methods used for smoothing the images before subtracting are not optimal, in the first method residuals may remain due to differences in the variable PSF, whereas in the second, flux conservation of a point source on a diffuse background is not guaranteed. The success of these techniques can only be judged by careful inspection of the subtracted frames.

We believe that by using both of these very different techniques, PSF fitting and template subtraction, we have a good chance of avoiding any systematic errors that might be inherent in these methods. We did not see any systematic differences between the two methods and the measured differences per epoch were typically less than 0.1 magnitudes. The magnitudes we present in Table 3 are consistent with both of the above mentioned methods except for the latest epoch, where only the template subtraction method was used. The supernova was clearly visible in these images, but the signal to noise was too low for reliable PSF fitting.

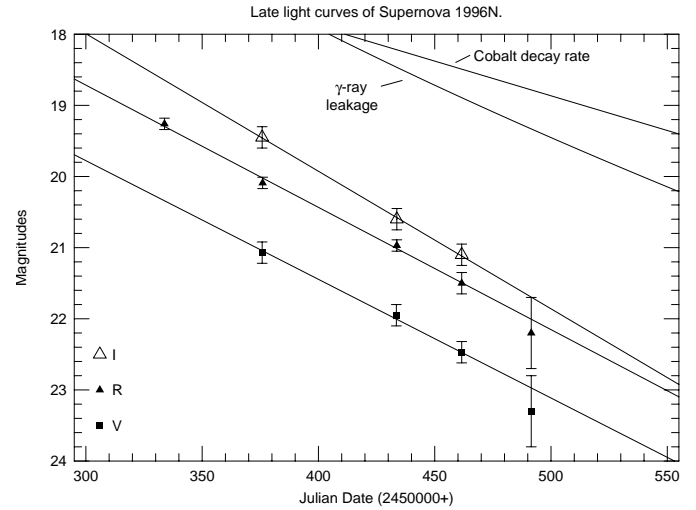


Fig. 2. The late light curves of SN 1996N. The lines are chi-square fits to the magnitudes and their errors. Also indicated is the decay rate for ^{56}Co , i.e., the lightcurve for full trapping of the γ -rays. The line labeled “ γ -ray leakage” refers to the model explained in the text. The supernova was discovered on March 12.5 UT, which corresponds to JD 2450155.

2.2. Spectroscopy

The log of our spectroscopic observations is shown in Table 4. With the exception of the January 1997 observation each spectrum is the combination of observations with two gratings to cover the blue and the red wavelength range. The slit was always oriented East-West. Since the supernova culminated close to zenith this was always close to the parallactic angle. Spectral reductions included bias subtraction and flat fielding, wavelength calibration with observations of arc lamps obtained immediately before or after the supernova observation, and flux calibration using standard stars (Hamuy et al. 1992). The typical accuracy of the wavelength calibration is between 0.5 and 1.0 Å, depending on the resolution provided by the grism. Some of the observations were obtained under non-photometric conditions, also slit losses might contribute to flux uncertainties. To establish the absolute fluxes for the spectra we convolved them with our simultaneous *R* photometry.

3. Results

Fig. 2 shows the late light curves of SN 1996N. We have compiled all our photometry here: five observations in *R*, four in *V* and three in *I*. The magnitudes decline linearly and chi-square fits to the magnitudes and their errors gives for the *R* lightcurve a slope of 1.72 ± 0.10 magnitudes per 100 days, between 179 days and 337 days past discovery. The *V* lightcurve has 1.67 ± 0.23 mag $(100\text{d})^{-1}$ whereas *I* has 1.93 ± 0.24 . Thus, we see no evidence for a strong color dependence in the decline.

An early spectrum of SN 1996N was obtained on March 23.4 at the AAT by L. Germany, B. Schmidt, R. Stathakis and H. Johnston (Germany et al. 1996). We have re-reduced and analyzed that spectrum and confirm the classification of SN 1996N as a

Table 3. Supernova Magnitudes.

Julian Dates 2450000+	V	R	I
333.8	...	19.26±0.08	...
375.9	21.07±0.15	20.09±0.08	19.45±0.15
433.7	21.95±0.15	20.97±0.08	20.6±0.15
461.6	22.5±0.15	21.5±0.15	21.1±0.15
491.5	23.3±0.5	22.2±0.5	...

Table 4. SN 1996N - log of spectroscopic observations.

Julian Date 2450000+	Phase ^a (days)	Telescope/ Instrument	Wavelength- range (Å)
333.8	178.8	3.6m/EFOSC1	3900-9700
376.0	221.0	2.2m/EFOSC2	4000-9100
433.7	278.7	2.2m/EFOSC2	4000-8700
461.6	306.6	2.2m/EFOSC2	4000-7900
491.5	336.5	3.6m/EFOSC1	3900-9700

^a Epochs in days past discovery, for the corresponding UT Date, see Table 1.

Type Ib/c. In fact, we identify three rather weak absorption lines as corresponding to He I $\lambda\lambda 5876, 6678$ and 7065 , all blueshifted by about 9000 km s^{-1} . This suggests that SN 1996N was of Type Ib. Apart from the helium lines we identify absorption lines of O I $\lambda 7774$ and the Ca II near-IR triplet.

The spectra of SN 1996N at five late epochs are shown in Fig. 3. The supernova was already entering its nebular phase at the first observation date, 179 days after discovery, and the lines of intermediate mass elements are clearly seen. The strongest lines are [O I] $\lambda\lambda 6300, 6364$, [Ca II] $\lambda\lambda 7291, 7324$, the Ca II near-IR triplet (probably mixed with [C I] $\lambda 8727$), Mg I $\lambda 4571$ and Na I $D \lambda 5893$. There is also O I at $\lambda 7774$ and perhaps [O I] at $\lambda 5577$. The feature at $\sim 5300 \text{ \AA}$ is a mixture of Fe II emission. Fe II is also seen in the absorption dips at $\lambda\lambda 5018, 5169$.

All the emission lines are quite broad, [O I] $\lambda\lambda 6300, 6364$ shows a total FWHM of $\sim 6000 \text{ km s}^{-1}$ 179 days after discovery, the [Ca II] $\lambda\lambda 7291, 7324$ is somewhat narrower with a FWHM of $\sim 4600 \text{ km s}^{-1}$.

A smaller velocity for calcium than for oxygen is consistent with most explosion models, where Ca is produced further in than O. In SN Ib/c 1985F these lines had about the same velocities (Schlegel & Kirshner 1989) and in SN Ic 1994I, [Ca II] was even broader than [O I] (Filippenko et al. 1995). Some caution is, however, necessary in interpreting the widths of these lines, as they are both blends. We tried to deconvolve these blends using Gaussian line shapes, and our fits indicate that the [O I] lines were indeed broader. The best fits were obtained for a FWHM of $\sim 4500 \text{ km s}^{-1}$ for [Ca II] and $\sim 5200 \text{ km s}^{-1}$ for [O I], where we used an optically thin line ratio of 3:1.

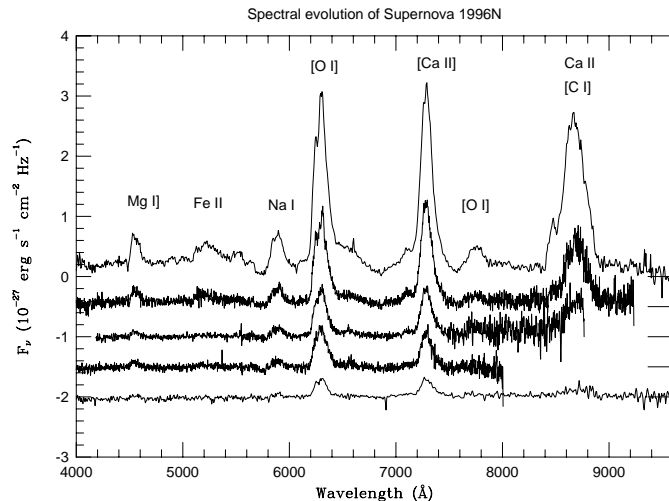


Fig. 3. The spectral evolution of SN 1996N. The wavelength scale has been corrected for the redshift of NGC 1398. The flux scale refers to the uppermost spectrum, the first date of observation. The tick marks to the right indicate the zero levels for the fluxes. The strongest emission lines have been identified.

For comparison, SN Ib/c 1985F had a FWHM of $\sim 4700 \text{ km s}^{-1}$ for [Ca II] $\lambda\lambda 7291, 7324$ at 300 days (Schlegel & Kirshner 1989). Similarly, SN Ib 1993J had $\sim 4600 \text{ km s}^{-1}$, but SN II 1986I had only $\sim 2600 \text{ km s}^{-1}$ at similar epochs (Filippenko et al. 1994). SNe Ic 1987M and 1994I showed even higher velocities, 6200 km s^{-1} and 9200 km s^{-1} respectively, at about 4.6 months (Filippenko et al. 1995). The higher velocities in SNe Ib/c are usually attributed to their smaller masses. For any given explosion energy, a smaller mass of the ejecta allows for larger velocities.

In Table 5 we present the evolution of the fluxes for the stronger emission lines. These fluxes are rather uncertain, especially for the later spectra, and the errors could be as large as 50%. Line ratios for lines with a large wavelength separation might be affected by additional uncertainties, like reddening and slit losses. Most line ratios seem to stay rather constant during this epoch, although the Ca II near IR triplet appears to be getting weaker compared to [Ca II] $\lambda\lambda 7291, 7324$. This was also noticed in SN Ic 1987M, and interpreted as due to decreasing density (Filippenko et al. 1990). Table 5 also presents the FWHM and central wavelengths of the emission lines. These were simply estimated using Gaussian fits. The observed blueshifts will be discussed in Sect. 4.4.

No corrections for absorption have been applied. We have little handle on any absorption towards SN 1996N. We examined the early phase AAT spectrum for any signs of Na absorption at the redshift of NGC 1398, but the spectrum is of low signal and does not constrain the absorption. Our first spectrum from September 1996 has appreciable flux at the expected Na absorption, but it is also of low resolution and even a fairly strong, narrow Na absorption could not be detected. The HI maps do indicate that there is no absorption from our own Galaxy towards SN 1996N (Burstein & Heiles 1984). Even though absence of

Table 5. Emission lines

	Julian Dates (2450000+)				
	333.8	376.0	433.7	461.6	491.5
[O I] $\lambda\lambda$ 6300, 6364					
Flux (10^{-15} erg s^{-1} cm^{-2})	25.0	13.2	6.6	6.1	2.4
Central wavelength (\AA)	6293	6294	6294	6294	6295
FWHM (\AA)	126	128	123	129	116
[Ca II] $\lambda\lambda$ 7291, 7324					
Flux (10^{-15} erg s^{-1} cm^{-2})	17.4	9.6	4.8	3.2	1.7
Central wavelength (\AA)	7285	7285	7286	7283	7287
FWHM (\AA)	111	108	111	105	118
Na I D λ 5893					
Flux (10^{-15} erg s^{-1} cm^{-2})	6.0	2.4	1.5	1.1	0.5
Central wavelength (\AA)	5886	5888	5892
FWHM (\AA)	134	129	137
Mg I] λ 4571					
Flux (10^{-15} erg s^{-1} cm^{-2})	5.6	2.7	1.2	1.1	0.9
Central wavelength (\AA)	4554	4554	4553	4551	...
FWHM (\AA)	81	93	87	100	...
Ca II near-IR triplet					
Flux (10^{-15} erg s^{-1} cm^{-2})	25.4	9.4	1.0
Central wavelength (\AA)	8669	8685
FWHM (\AA)	244	226

The positions and FWHM are simply measured by Gaussian fits, the fluxes are, however, integrated over the whole line. Wavelengths are in the rest frame of NGC 1398, which has a recession velocity of 1407 ± 6 km s^{-1} (de Vaucouleurs et al. 1991).

evidence is not evidence for absence, we nevertheless have not applied any absorption corrections for what follows.

4. Discussion

4.1. The light curve

Along with the light curves in Fig. 2, we have also plotted the decay rate of ^{56}Co ; 0.98 mag $(100\text{d})^{-1}$. This is the slope the bolometric late light curve of a radioactively powered supernova would have if it trapped all of its γ -rays. Most SNe II follow this decay rate closely (Turatto et al. 1990; Patat et al. 1994). It is clear from Fig. 2 that the light curves of SN 1996N decline substantially faster.

SNe Ib/c seem to be able to display a variety of light curves. For example, SN Ib 1984L followed the ^{56}Co decay rate for at least ~ 500 days (Schlegel & Kirshner 1989), whereas SN 1994I, a Type Ic, faded even faster than SNe Ia, at least up to about 70 days after maximum (Richmond et al. 1996b). A well studied supernova with a fast decay rate is SN 1993J. In Fig. 4 we compare the V and R light curves of SN 1996N with the light curves of SN 1993J, taken from the La Palma archive (cf.

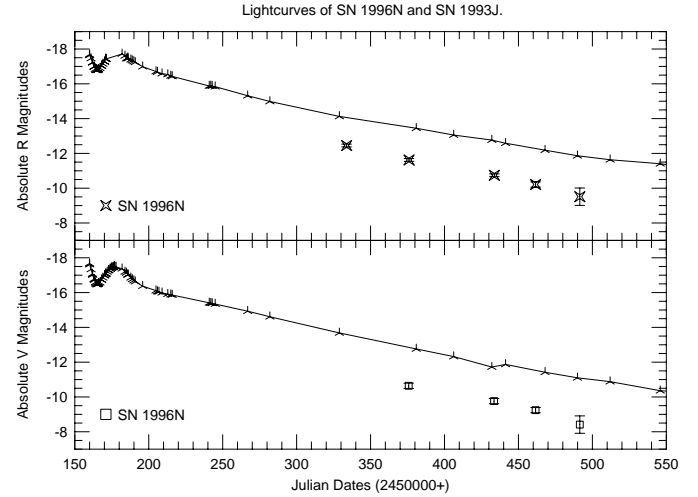


Fig. 4. Absolute lightcurves for SN 1996N and SN 1993J. We have used 22.0 Mpc for SN 1996N and applied no extinction correction for this supernova. For SN 1993J, 3.6 Mpc and $E(B - V) = 0.19$ were used. Uppermost panel is R data, and lowermost is V data. The Julian Dates refers to the SN 1996N photometry. The SN 1993J photometry have been shifted so that March 26.0, the inferred explosion date for SN 1993J, matches the discovery date of SN 1996N.

Lewis et al. 1994). It is clear from this figure that the light curve slopes of these supernovae are rather similar at late times.

It has been argued (Clocchiatti & Wheeler 1997) that there exists a homogeneous photometric group of SNe with light curve slopes of about 1.9 mag $(100\text{d})^{-1}$ after ~ 150 days. This group contains SN Ib 1993J as well as SN Ib 1983N and SN Ic 1983V. These SNe have similar late time slopes and peak to tail ratios. The similar photometric behaviour could perhaps indicate similar progenitors, where the early spectra, and thus the classification, is determined by small differences in the thin outer layers of the progenitors (Clocchiatti & Wheeler 1997).

The late time decline rate for SN 1996N is similar, but somewhat faster, than the decline of SN 1993J. A chi-square fit to the data of SN 1993J from the La Palma archive and from Richmond et al. (1996a) gives slopes for the V , R and I light curves of 1.53 ± 0.03 , 1.36 ± 0.06 , and 1.43 ± 0.12 mag $(100\text{d})^{-1}$ respectively, between 170 and 340 days after explosion.

As the filter light curves of SN 1996N all have the same slope, within the errors, a linear scaling to bolometric luminosity seems justified. For the three epochs where we have V , R and I photometry the summed fluxes show a decline rate of 1.75 ± 0.25 mag $(100\text{d})^{-1}$. The fast decline of the optical light curves of SN 1996N thus indicates leakage of γ -rays from the ^{56}Co decay.

A very simplified model of γ -ray deposition in an expanding homogeneous sphere predicts a slope of $1.09 \times (111.3^{-1} + 2\text{t}^{-1})$ magnitudes per day for late times, when the optical depth $\tau \ll 1$ (Clocchiatti & Wheeler 1997). Here, 111.3 days is the e-folding time for the radioactive decay of ^{56}Co . For the epochs of observation for SN 1996N, this gives a slope of 1.9 mag $(100\text{d})^{-1}$, very similar to the measured value of 1.7 mag $(100\text{d})^{-1}$. The similarity of the light

curve slopes of many supernovae at these late epochs may thus simply reflect the asymptotic behaviour of the γ -deposition, reached when the optical depth for γ -rays becomes very low (Clocchiatti & Wheeler 1997).

If the optical depth for γ -rays is in fact very low, the contribution from positrons must be taken into account. For a simplified model with a central radioactive source (Sollerman et al. 1998) the bolometric luminosity decays as $e^{-t/111.3} (1 - 0.965 e^{-\tau})$, where 111.3 days is again the decay time of ^{56}Co , 96.5 % of the energy is mediated by γ -rays and the rest by positrons. The positrons are assumed to deposit their energy locally while the γ -rays have an optical depth $\tau=(t/t_1)^{-2}$, where t_1 is the time when $\tau=1$. In this model, a slope of 1.7 ± 0.2 mag $(100 \text{ days})^{-1}$ between 179 and 337 days past explosion can be achieved for $t_1=63 - 218$ days. In fact, the steepest decline is 1.67 mag $(100\text{d})^{-1}$ for $t_1=121$ days, this slope is also shown in Fig. 2. Within this model, it seems that SN 1996N was declining as fast as it could.

As seen from the absolute light curves in Fig. 4, SN 1996N appears to be fainter than SN 1993J. The distance to SN 1993J is well determined from Cepheids as 3.6 Mpc (Freedman et al. 1994) and estimates for the reddening of SN 1993J ranges from $E(B - V)=0.08$ to 0.4 (Barbon et al. 1995). Here we have adopted $E(B - V)=0.19$ from Lewis et al. (1994). The distance to NGC 1398 is about 22.0 Mpc for $H_0=65 \text{ km s}^{-1} \text{ Mpc}^{-1}$ (Kraan-Korteweg 1986), and we have assumed in Fig. 4 that there was no intrinsic extinction for SN 1996N. An error of ± 0.5 magnitudes due to current uncertainties in H_0 , and another 0.25 mag allowing for an uncertainty of two weeks in the date of explosion for SN 1996N, is not enough to resolve the difference shown in Fig. 4.

This indicates that SN 1996N was underluminous compared to SN 1993J, or that the intrinsic extinction for SN 1996N was as high as $E(B - V)=0.8\pm 0.3$. As these supernovae have similar light curve declines, the faintness of SN 1996N could be due to a substantially lower mass of ejected ^{56}Ni (cf. Sollerman et al. 1998).

4.2. The mass of oxygen

The mass of oxygen in the supernova is potentially interesting as the amount synthesized in supernova models is rather sensitive to the core mass. For example, in a model with a helium core of $3.3 M_\odot$, $0.22 M_\odot$ of oxygen is synthesized, while a core of $6 M_\odot$ gives $1.5 M_\odot$ (Thielemann et al. 1996).

Assuming that the electron density $n_e \geq 10^6$, which is quite reasonable for these epochs (Schlegel & Kirshner 1989), one can use the luminosity of the [O I] $\lambda\lambda 6300, 6364$ lines to estimate the mass of oxygen (or rather of neutral oxygen), using $M_o = 10^8 d^2 F([\text{O I}]) e^{2.28/T_4}$ (Uomoto 1986). Here M_o is the mass of oxygen in solar masses, d is the distance to the supernova in Mpc, F is flux in $\text{erg s}^{-1} \text{ cm}^{-2}$ and T_4 is the temperature in units of 10^4 K. This estimate assumes these emission lines to be optically thin. We were not able to constrain the density from the [O I] $\lambda\lambda 6300, 6364$ lines, although a normal 3:1 ratio seems to give the best deconvolution of the blend. Neverthe-

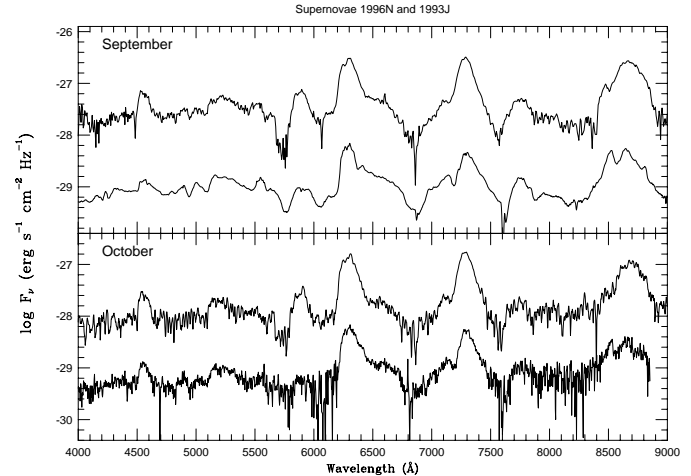


Fig. 5. Late time spectra of SN 1996N and SN 1993J. Uppermost panel shows SN 1996N (above) from Sep. 7, 1996, 179 days past discovery. Below is a spectrum of SN 1993J retrieved from the La Palma database. It was taken on Sep. 20, 1993, 176 days after discovery. The lower panel shows SN 1996N, 221 days past discovery (above) and SN 1993J, 224 days past discovery (below). The flux scales are for SN 1996N, the spectra of SN 1993J have been shifted by 3.5 dex.

less, a lower limit to the oxygen mass can be achieved using this method.

The temperature can be constrained by the [O I] $\lambda 5577$ / [O I] $\lambda\lambda 6300, 6364$ ratio. Assuming that all the emission seen at $\sim 5530 \text{ \AA}$ in our earliest spectrum is due to [O I] $\lambda 5577$, we find a ratio < 0.08 . This is rather similar to the values found for SN 1985F and SN 1983N, 0.05 and 0.04 respectively (Gaskell et al. 1986). This constrains the temperature for $n_e = 10^8 - 10^9 \text{ cm}^{-3}$ to be $T < 5000 - 4400 \text{ K}$, which in turn gives $M_o > 0.11 - 0.21 M_\odot$, for a distance of 22.0 Mpc. The lower value of the oxygen mass corresponds to the lower density. The O I $\lambda 7774$ line also indicates the presence of ionized oxygen, as this line presumably comes from recombination (Begelman & Sarazin 1986). This would increase the estimated total mass of oxygen.

These estimates are, however, rather sensitive to uncertainties in the distance and reddening. The distance above comes from Kraan-Korteweg (1986), using a value of $65 \text{ km s}^{-1} \text{ Mpc}^{-1}$ for H_0 . An uncertainty of $\pm 15 \text{ km s}^{-1} \text{ Mpc}^{-1}$ in that number transforms to $M_o > 0.11_{-0.04}^{+0.09}$ for $n_e = 10^8$ and $M_o > 0.21_{-0.07}^{+0.16}$ for $n_e = 10^9$.

These values are not very different from the estimates obtained for SN II 1986J (Leibundgut et al. 1991), $0.1 < M_{\text{O I}} < 0.3 M_\odot$. Houck & Fransson (1996) argued that the oxygen mass in SN 1993J was $0.5 M_\odot$.

4.3. The spectra - evidence for hydrogen?

The spectra of SN 1996N at late times are similar to those of other SNe Ib/c in the nebular phase (Filippenko et al. 1990; Filippenko 1997). In particular, they resemble the spectra of SN 1993J (Fig. 5). Note the broad feature at the red side of the [O I] $\lambda\lambda 6300, 6364$, which in SN 1993J was attributed to $\text{H}\alpha$.

Here we want to discuss if the same identification can be made for SN 1996N.

SN 1993J showed hydrogen in its early spectra but underwent a spectroscopic metamorphosis to a SN Ib/c in nebular phase, where the rather weak, broad $H\alpha$ remained the only evidence for the SN II origin. A similar transformation was seen in SN 1987K (Filippenko 1988) and more recently in SN 1996cb (Garnavich 1997), which displayed a spectral evolution similar to that of SN 1993J.

If the emission redward of [O I] $\lambda\lambda 6300, 6364$ in SN 1996N is to be interpreted as broad $H\alpha$, as it was in SN 1993J, one must thus address the question why no $H\alpha$ was seen in the early spectrum of SN 1996N. Remembering that the $H\alpha$ absorption in SN 1993J was very weak, it is tempting to assume that this feature could be totally lost for SNe with even less hydrogen. Perhaps the only early spectrum for SN 1996N was taken at an epoch when the thin hydrogen layer had already recombined.

However, the faint, broad $\sim 6600 \text{ \AA}$ feature seen in the late spectrum of SN 1983N (Gaskell et al. 1986) indicates that this might be a more common scenario. SN 1983N was rather well studied at early times (Harkness et al. 1987), and showed no prominent $H\alpha$ absorption in its early spectra, hence the Type Ib classification.

Spectral modeling by Wheeler et al. (1994) showed the early spectrum of SN 1983N to be consistent with the presence of small amounts ($\sim 0.005 M_{\odot}$) of hydrogen. For SN 1993J, Swartz et al. (1993) concluded that $0.04 M_{\odot}$ of hydrogen could reproduce the early spectra. This indicates that only very small amounts of hydrogen could in fact be hidden in the early spectra of SNe Ib/c. However, none of these studies did investigate a broad range of hydrogen abundances or distributions.

Unfortunately, it is not trivial to estimate if such a small amount of hydrogen is able to produce the observed emission at late times. A simple-minded way is to assume that all the emission comes from case B recombination with $T=10\,000 \text{ K}$. Then

$$M(H^+) = 0.5 \varepsilon^{0.5} \left(\frac{V}{10\,000 \text{ km s}^{-1}} \right)^{1.5} \left(\frac{t}{179 \text{ days}} \right)^{1.5} \\ \left(\frac{f}{10^{-14} \text{ erg s}^{-1} \text{ cm}^{-2}} \right)^{0.5} \left(\frac{d}{22 \text{ Mpc}} \right) \left(\frac{n_p}{n_e} \right)^{0.5}$$

$M(H^+)$ is the mass of ionized hydrogen in solar masses, ε is the filling factor, V is the maximum velocity of the hydrogen shell in km s^{-1} , t is time since explosion measured in days, f is the flux of $H\alpha$ in $\text{erg s}^{-1} \text{ cm}^{-2}$, d is the distance to the supernova in Mpc and $(\frac{n_p}{n_e})$ is the ratio of protons to electrons. We estimated the flux in the $H\alpha$ line to be $\sim 8 \times 10^{-15} \text{ erg s}^{-1} \text{ cm}^{-2}$ in our earliest spectrum, by measuring the red unblended part of the line and assuming that it is symmetric. The line extends to $\sim 10\,000 \text{ km s}^{-1}$, assuming it is blueshifted by the same amount as [Ca II] $\lambda\lambda 7291, 7324$. These numbers give, for an epoch of 179 days, a required mass of ionized hydrogen of $0.5 \varepsilon^{0.5} (\frac{n_p}{n_e})^{0.5} M_{\odot}$. If the hydrogen is really uniformly distributed this estimate is quite high, and seem diffi-

cult to reconcile with the lack of hydrogen in the early spectrum. The hydrogen is, however, likely to be distributed in a narrow shell, and the distribution is probably very clumpy. If the hydrogen would be distributed in a shell between $8000 - 10\,000 \text{ km s}^{-1}$, with a filling factor $\varepsilon=0.01$, we would instead get $M(H^+)=0.02 (\frac{n_p}{n_e})^{0.5} M_{\odot}$. Such a low mass of hydrogen is perhaps not in conflict with early time spectra.

If the discussed feature is indeed $H\alpha$, it must somehow be excited at these late epochs. An obvious suggestion is ionization by the X-rays from the shock between the ejecta and the CSM. After all, SNe Ib/c and transition objects like SN 1993J are believed to be core-collapse supernovae with progenitors which lost much of their envelopes before the explosion. Evidence for circumstellar interaction comes from radio observations; SN 1993J, SN 1996cb as well as SNe Ib 1983N and 1984L were, just as SN 1996N, detected at radio wavelengths (Weiler et al. 1998). Furthermore, the broad $H\alpha$ line in SN 1993J was powered by circumstellar interaction after ~ 250 days (Houck & Fransson 1996; Patat et al. 1995).

However, for a constant mass loss rate, CSM density profile and ejecta density profile, the X-ray luminosity from a radiative reverse shock, and thus the $H\alpha$ emission, is expected to stay rather constant with time, as was seen after ~ 300 days in SN 1993J. In SN 1996N this is not observed.

An alternative suggestion for the excitation of $H\alpha$ in the late time spectra of SN 1996N is line blending with [O I] $\lambda 6364$. This was in fact shown to be the most important mechanism for populating $n=3$ in SN 1993J at this epoch (Houck & Fransson 1996).

If the discussed emission line is not $H\alpha$, we must postulate the existence of a broad blend of emission lines at $\sim 6600 \text{ \AA}$. This was suggested by Patat et al. (1995) for SN 1993J, were this blend possibly contributed 30% of the emission at the position of $H\alpha$. A broad blend, attributed to Fe II, is seen in early time spectra of SN Ia. This feature is indeed sometimes incorrectly identified as $H\alpha$ (Filippenko 1997). We would then be left with the annoying fact that very similar spectral features can be due to very different physics. We must also try to understand why the $\sim 6600 \text{ \AA}$ bump is so prominent in SN 1996N, compared to other SNe Ib/c.

The ongoing discussion on the nature of SNe Ib/c, and especially of their progenitors, has been focused on the presence or absence of hydrogen (and helium) in their early spectra, see the review by Filippenko (1997). Based on the resemblance of the spectra of SN 1996N and SN 1993J, we can speculate whether small amounts of hydrogen might go unnoticed in early spectra of SN Ib/c. Later on, when the SN continuum has faded, this hydrogen shell might be reionized by CSM interaction, or excited via line blending, thus revealing its existence. Late time spectra might then be the best way to resolve this issue.

4.4. The blueshifts of the emission lines

As indicated in Table 5, the emission lines of SN 1996N appear to be blueshifted with respect to the parent galaxy, the velocities inferred are $\sim 1000 \text{ km s}^{-1}$. This is, again, similar to the case of SN 1993J, were the blueshifts of the oxygen lines attracted at-

tention by several authors. Many different models were put forward to explain the blueshifts in SN 1993J: Wang & Hu (1994) proposed that in a clumpy distribution, only the approaching clumps would be seen due to their proximity to the photosphere. Similarly, Filippenko et al. (1994) proposed that the blueshifts were due to optically thick ejecta, where we view only the approaching side. A different explanation was suggested by Spyromilio (1994), who interpreted the lineshifts as indications for large scale asymmetries in the distribution of the ejecta. This scenario was also suggested by Lewis et al. (1994). Finally, Houck & Fransson (1996) proposed that the lineshifts were simply an effect of line blending.

There were difficulties in all of these models for SN 1993J. The emission lines did not show the same amount of blueshift. For example, in the spectrum from September 20, 1993, shown in Fig. 5, we measured the blueshift of [O I] $\lambda 5577$ to be $\sim 1500 \text{ km s}^{-1}$ whereas [Ca II] $\lambda 7308$ only shows a shift of $\leq 300 \text{ km s}^{-1}$. It is difficult to understand how optical depth effects can affect these lines so differently. Moreover, such scenarios would predict the lineshifts to decrease with time, as the optical depth decreases. On the contrary, the shifts seemed unchanging in nature (Lewis et al. 1994; Spyromilio 1994).

Similarly, the case for large scale asymmetries in the ejecta mass have a problem in explaining the much smaller blueshift of O I $\lambda 7774$, as pointed out by Houck & Fransson (1996). This line seems to be blueshifted by only $\sim 500 \text{ km s}^{-1}$, significantly less than the [O I] $\lambda 5577$ line. This led Spyromilio (1994) to suggest that also the distribution of ^{56}Co was asymmetric, explaining the spatial differences in excitation conditions.

Houck & Fransson (1996) used a detailed spectral modeling code to conclude that no large scale asymmetries were required to reproduce the spectra of SN 1993J. Instead, they argued that the apparent blueshifts could be explained as effects of line blending. For example, the blueshift of the [O I] $\lambda\lambda 6300, 6364$ line could be due to blending with fast-moving hydrogen. They further proposed that the shifts of Mg I $\lambda 4571$ and [O I] $\lambda 5577$ could be explained along the same line. However, the O I line at 7774 \AA seems to be rather unaffected by line blending. The blueshift of this line in SN 1993J might thus indicate real large scale asymmetries.

For SN 1996N, blueshifts of the order of 1000 km s^{-1} were observed for [O I] $\lambda\lambda 6300, 6364$, [Ca II] $\lambda\lambda 7291, 7324$ and Mg I $\lambda 4571$. The actual numbers given in Table 5 are rather uncertain, they merely reflect Gaussian fits to these non-Gaussian lines. These fits do, however, indicate systematic blueshifts of the emission lines, and show that these stay rather constant with time. That the lines are indeed shifted can be seen from Fig. 6, where the above mentioned lines, as well as O I $\lambda 7774$, are plotted in velocity space. Furthermore, as shown in Fig. 7, no evolution in the widths or positions of the emission lines is seen between 179 and 337 days past discovery. As the density is expected to decrease by a factor of ~ 7 between our first and last spectrum, an evolution of the line centers towards the rest positions would have been expected, if the shifts were due to optical depth effects. The scenario of Houck & Fransson may provide some clues to the observed blueshifts in SN 1996N. In

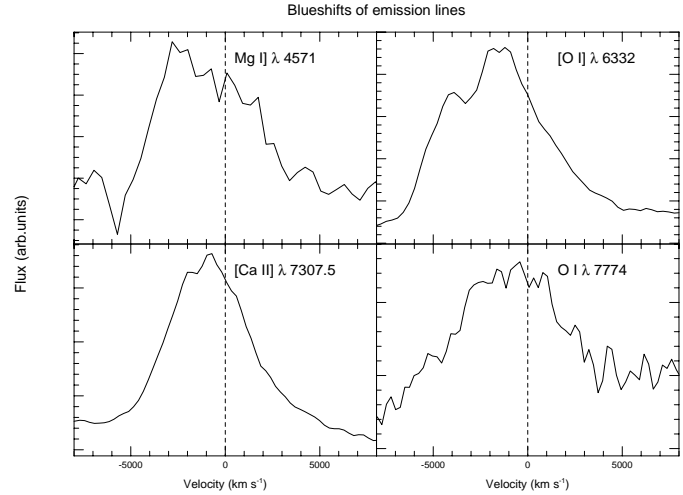


Fig. 6. Emission lines from the spectrum taken on September 7, 1996. The x-axis is velocity with respect to the indicated rest wavelengths within NGC 1398. It is clear that all these lines show significant blueshifts.

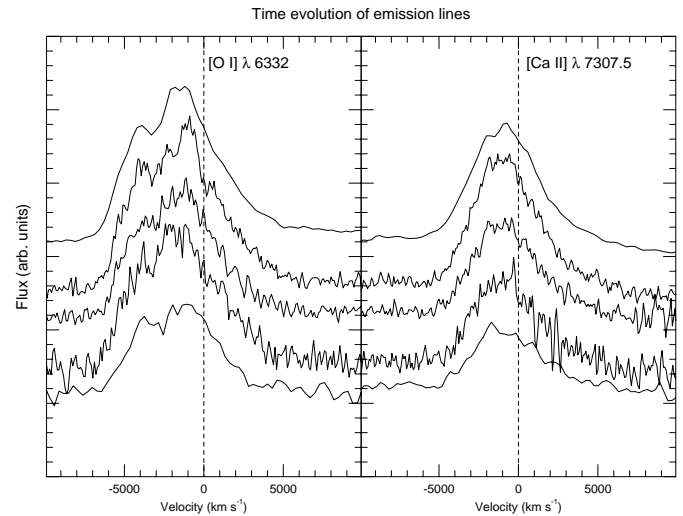


Fig. 7. Time evolution of the two strongest emission lines. Uppermost spectrum is our earliest observation from September 7, 1996. The others are in chronological order, dates can be read from Table 3. No evolution of the blueshifts or widths of these lines is seen.

particular, if we identify the emission redward of [O I] $\lambda 6364$ as $\text{H}\alpha$, as suggested in the previous section, the same scattering effect may be at work also in SN 1996N. We do, however, see a significant blueshift also in the [Ca II] $\lambda\lambda 7291, 7324$ lines, which was not noticed in SN 1993J. Furthermore, the O I $\lambda 7774$ line is positioned at $\sim 7749 \text{ \AA}$ in our earliest spectrum. The line is rather weak and broad but is clearly shifted to the blue by $\sim 800 - 1000 \text{ km s}^{-1}$ (Fig. 6). Again, this line is supposed to be relatively unblended, and the blueshift we observe might therefore correspond to real asymmetries in the distribution of the ejecta mass.

Another possible explanation for the blueshifts of the emission lines is dust. In SN 1987A, the emission lines slowly departed to the blue after ~ 500 days, an effect attributed to

dust formation (Lucy et al. 1989). The shifts in SN 1987A were $\sim 600 \text{ km s}^{-1}$. To achieve velocity shifts of $\geq 1000 \text{ km s}^{-1}$, optical depths for the dust in excess of $\tau=0.5$ are needed for an ejecta velocity of 5000 km s^{-1} . We do not observe any dependence of the line shifts on wavelengths, as seen for the dust extinction in SN 1987A. In particular, the $\text{Na I } D \lambda 5893$ line seems to be less blueshifted than all other lines. Also, our first observation is at 179 days, much earlier than the epoch of dust formation in SN 1987A. The temperature may well be too high for dust formation at this early stage. Similarly, in SN 1993J the shifts were observed already 50 days past maximum. We therefore consider this scenario less likely.

Finally we would like to mention the fact that many supernova remnants show emission lines with large ($\sim 500 \text{ km s}^{-1}$) velocity shifts. Also the high space velocities of pulsars are well known. These phenomena are often suggested to be due to asymmetric supernova explosions. Perhaps this is what we see here, for the supernova itself.

5. Conclusions

We have studied the Type Ib SN 1996N both photometrically and spectroscopically at rather late phases. The optical light curves decline substantially faster than the decay rate of ^{56}Co , indicating leakage of γ -rays. The light curve slopes seem similar, but somewhat steeper, than the light curves of SN 1993J. Unless SN 1996N is heavily reddened, it is underluminous compared to SN 1993J. The spectra of SN 1996N are strikingly similar to those of SN 1993J. In particular, it is tempting to identify the broad red wing of $[\text{O I}] \lambda 6364$ with $\text{H}\alpha$ also in SN 1996N. The presence of $\text{H}\alpha$ in the late spectrum of a SN Ib would further strengthen the belief that SN II and SN Ib/c are just variations of the same core collapse theme. Finally, the substantial blueshifts of the emission lines of SN 1996N may be an indication of large scale asymmetries in the ejecta. Further studies of core-collapse SNe at late epochs will clarify how common the phenomena discussed in this paper are.

Acknowledgements. We thank L. Germany, B. Schmidt, R. Stathakis and H. Johnston for sending us the raw data on the early spectrum, P. Schechter for help with DoPhot and R. Hook for advise on image analysis. We also thank G. Contardo for help with L_{VRI} and P. Lundqvist for interesting discussions on CSM interaction. We are grateful to the La Palma observatory & Royal Greenwich Observatory for the possibility to access their SN 1993J database by ftp, and we thank the NTT service observation team for nice service observations. J. Sollerman is grateful to the ESO Studentship that allowed his stay in Garching, where this work was conducted.

References

- Barbon, R., Benetti, S., Cappellaro, E., et al. 1995, A&AS 110, 513
 Begelman, M. C., Sarazin, C. L. 1986, ApJ 302, L59
 Burstein, D., Heiles, C. 1984, ApJS 54, 33
 Clocchiatti A., Wheeler, J. C. 1997, ApJ 491, 375
 Filippenko, A. V., 1988, AJ 96, 1941
 Filippenko, A. V., 1997, ARA&A 35, 309
 Filippenko, A. V., Porter, A. C., Sargent, W. L. W. 1990, AJ 100, 1575
 Filippenko, A. V., Matheson, T., Barth, A. J. 1994, AJ 108, 2220
 Filippenko, A. V., Barth, A. J., Matheson, T., et al. 1995, ApJ 450, L11
 Freedman, W. L., Hughes, S. M., Madore, B. F., et al. 1994, ApJ 427, 628
 Garnavich, P. 1997, private communication
 Gaskell, C. M., Cappellaro, E., Dinerstein, H. L., et al. 1986 ApJ 306, L77
 Germany, L., Schmidt, B. P., Stathakis, R., Johnston, H. 1996, IAU circ. No. 6351
 Graham, J. A. 1982, PASP 94, 244
 Hamuy, M., Walker, A. R., Suntzeff, N. B. 1992, PASP, 104, 53
 Harkness, R. P., Wheeler, J. C. 1990, in Supernovae, ed. A. G. Petscheck (New York:Springer)
 Harkness, R. P., Wheeler, J. C., Margon, B., et al. 1987, ApJ, 317, 355
 Houck, J. C., Fransson, C. 1996, ApJ, 456, 811
 Kraan-Korteweg, R. C. 1986, A&AS, 66, 255
 Landolt, A. U. 1992, AJ 104, 340
 Leibundgut, B., Kirshner, R. P., Pinto, P. A., et al. 1991, ApJ, 372, 531
 Lewis, J. R., Walton, N. A., Meikle, W. P. S., et al. 1994, MNRAS 266, L27
 Lucy, L. B., Danziger, I. J., Gouiffes, G., Bouchet, P. 1989, In Structure and Dynamics of the Interstellar Medium, ed. G. Tenorio-Tagle et al., IAU Colloquium No. 120 (Springer-Verlag)
 Magain, P., Surdej, J., Vanderriest, C., et al. 1992, Messenger 67, 30
 Nomoto, K., Yamaoka, H., Pols, O. R., et al. 1994, Nat 371, 227
 Patat, F., Barbon, R., Cappellaro, E., Turatto, M. 1994, A&A 282, 731
 Patat, F., Chugai, N., Mazzali, P. A., 1995, A&A 299, 715
 Richmond, M. W., Treffers, R. R., Filippenko, A. V., Paik, Y. 1996a, AJ 112, 732
 Richmond, M. W., Van Dyk, S. D., Ho, W., et al. 1996b, AJ 111, 327
 Schechter, P. L., Mateo, M., Saha, A. 1993, PASP 105, 1342
 Schlegel, E. M., Kirshner, R. P. 1989, AJ 98, 577
 Swartz, D. A., Clocchiatti, A., Benjamin, R., et al. 1993, Nat 365, 232
 Sollerman, J., Cumming, R. J., Lundqvist, P. 1998, ApJ 493, 933
 Spyromilio, J. 1994, MNRAS 266, 61
 Thielemann, F. K., Nomoto, K., Hashimoto, M. 1996, ApJ 460,408
 Turatto, M., Cappellaro, E., Barbon, R., et al. 1990, AJ 100, 771
 Turatto, M., Cappellaro, E., Benetti, S., Danziger, J. I. 1993, MNRAS 265, 471
 Uomoto, A. 1986, ApJ 310, L35
 Van Dyk, S., Sramek, R. A., Weiler, K. W., et al. 1996, IAU Circ. No. 6351
 de Vaucouleurs, G., de Vaucouleurs, A., Corwin JR, H. G., et al. 1991, third reference catalogue of bright galaxies
 Wang L., Hu, J. 1994, Nat 369, 380
 Weiler, K. W., Van Dyk, S. D., Montes, M. J., et al. 1998, ApJ, in press
 Williams, A., Martin, R. 1996, IAU Circ. No. 6351
 Wheeler, J. C., Harkness, R. P. 1989, University of Texas, Dep. of Astronomy
 Wheeler, J. C., Harkness, R. P., Clocchiatti, A., et al. 1994, ApJ 436, L135
 Woosley, S. E., Langer, N., Weaver, T. A. 1993, ApJ 411, 823